SECED 2023 Conference
Earthquake Engineering & Dynamics for a Sustainable Future
14-15 September 2023, Cambridge, UK

AN EXAMPLE OF ASSESSING SEISMIC RESILIENCE FOR A HIGHWAY: CURRENT CAPABILITIES AND OPPORTUNITIES FOR IMPROVEMENT

Akrivi CHATZIDAKI[1], Chris GIANNELOS[2], Angeliki GERONTATI[3], Dimitrios VAMVATSIKOS[4], Marianna LOLI[5] & Angelos TSATSIS[6]

Abstract: *The seismic resilience is assessed for the Metsovo-Panagia segment of the Egnatia highway in Greece. It comprises long tunnels, steep slopes that are prone to landslides, bridges and the operator control building that are vulnerable to the seismic hazard. The aim is to develop a tool for pre-event risk assessment and rapid post-event inspection of critical road infrastructure by combining hazard, vulnerability, and sensor information to predict the resulting consequences. To enhance the assessment resolution, a component-based approach is adopted for the critical assets of the highway that allows evaluating damage scenarios for individual asset components (such as piers and bearings of a bridge) and propagate them to the asset-level performance. The asset interdependencies are considered to assess the system-level consequences for the entire highway, which are quantified in terms of repair losses, downtime, traffic delays and traffic capacity losses, the latter identified as the number of closed lanes and the allowable speed limit for the open ones. This allows tracing back the consequences after an event to individual assets to help road operators establish inspection prioritization protocols and manage associated incidents, facilitating the rapid assessment of the state of the highway and optimal recovery to full functionality. In light of such capabilities, we explore further improvements that can be reached for short/long-term assessments.*

Introduction

Nowadays road operators are facing the challenge of efficient maintenance and operation of road infrastructure networks as well as rapid inspection and recovery after catastrophic events. To this scope, researchers have focused on quantifying risk and resilience for interdependent highway networks. Risk assessment aims to assess the probability of occurrence of an undesirable event as well as the associated consequences (e.g., Kappos et al. 2014). Resilience goes a step further as it incorporates the dimension of time, aiming to determine the follow-up to a failure, i.e., to quantify the ability of the system to recover after the event. Conceptual views of infrastructure resilience have been offered by researches (e.g. Cimellaro et al. 2010, Ouyang et al. 2012, Argyroudis at al. 2019), with some of them focusing on road infrastructure networks under seismic hazard (e.g., Costa 2018, Kilanitis and Sextos 2019). Still, the definition and application of a practical approach for resilience assessment that allows quantifying the follow-up to a failure at every step of a system's recovery back to full functionality, remains a challenge.

To this scope, seismic resilience assessment of highway networks is integrated with real-time sensor information to offer a tool for pre-event assessment and rapid post-event inspection of critical road infrastructure. This is incorporated in a holistic decision support tool that can help road operators efficiently inspect, maintain, and safely operate road infrastructure networks, efficiently mitigating and managing risks. Staring from individual assets, the principles of performance-based earthquake engineering (Cornell and Krawinkler 2000) are followed, i.e., the seismic hazard is convolved with fragility and consequence functions to quantify risk. Specifically, the Multi-Stripe Analysis (MSA, Jalayer and Cornell 2009) results that provide information on the asset's structural response are combined with the asset's fragility curves to allow estimating the

[1] PhD Student, School of Civil Engineering, National Technical University of Athens, Athens, Greece, cakrivi@central.ntua.gr
[2] PhD Student, School of Civil Engineering, National Technical University of Athens, Athens, Greece
[3] PhD Student, School of Civil Engineering, National Technical University of Athens, Athens, Greece
[4] Associate Professor, School of Civil Engineering, National Technical University of Athens, Athens, Greece
[5] Researcher, Grid Engineers, Athens, Greece
[6] Researcher, Grid Engineers, Athens, Greece

expected damages. Damage-to-consequence functions are employed to translate damage into the consequences in terms of losses, downtime, and actions that the road operator should take, i.e., close any lanes and/or reduce the speed limit in the remaining open ones. The results are represented by numerous event-consequence scenarios that allow accommodating rapid damage and consequence identification. To this scope, enhanced resolution is adopted for the critical highway assets that allow tracing back potential consequences to individual components with more ease, in order to facilitate the rapid inspection. The asset-level consequences are propagated to the entire system by considering the asset-to-system interdependencies, aiming to assess the system-level impact in terms of monetary losses, downtime, traffic delays and system's recovery back to full functionality.

Recovery is estimated by combining the number of lanes that may be closed after an event, the speed limit in the open ones, and the time needed for concluding repair actions using a pre-defined recovery shape. Cimellaro et al. (2006) proposed adopting a linear, trigonometric or exponential recovery function depending on the response of the system and the operator, while more complicated shapes have also been proposed in literature (e.g., Miles and Chang 2006, Zhang et al. 2017). In our case, for any single asset, the "bathtub" recovery function of Figure 1a is adopted that starts at 100% capacity before the event. The event causes a drop to a lower capacity level (fewer cars allowed through) due to a reduction in the speed limit and/or potential lane closure that is required for inspection and damage fixing. All such restrictions are lifted and the full traffic capacity of the asset is restored only when all repair actions are concluded and the damages are fixed. The system-level recovery is determined by assuming that repair actions are performed in parallel following the schema of Figure 1b. Specifically, for highway segments of limited length, the speed limit for the entire segment at every time instant during the system's recovery back to full functionality equals the minimum allowable speed limit imposed by the repair of all damaged assets.

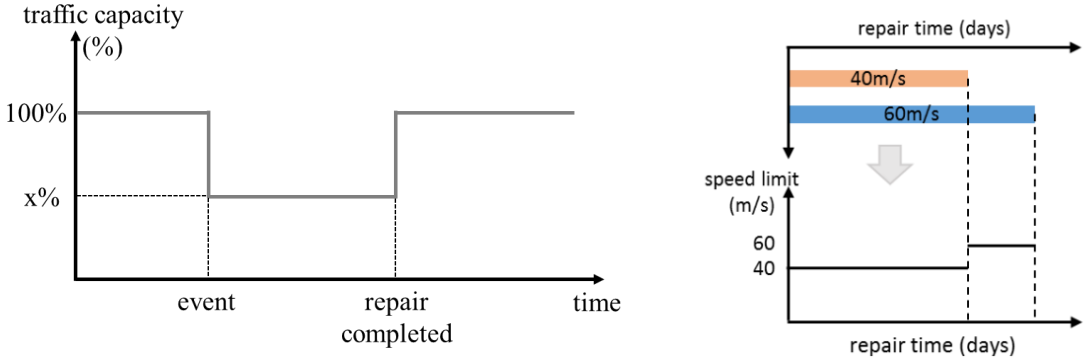

(a) (b)

Figure 1. (a) "Bathtub" recovery function, showing that the speed limit is reduced after a catastrophic event and is restored to its initial value when repair actions are completed, and (b) determining the speed limit at the system level over time by taking the minimum allowable to repair individual assets or components.

Herein, the risk and resilience assessment framework is demonstrated using the Metsovo-Panagia segment of Egnatia Odos in Greece as the case study (Figure 2). It comprises long bridges, tunnels and steep slopes in a high-altitude environment located in a moderately seismic area of Greece. The total length of the segment is 16km, while there is no alternative road within the Metsovo-Panagia segment that would allow a detour of vehicles. The only theoretically viable option is an old unmaintained road outside this segment as shown in Figure 2, although there is a great chance that it will be even more damaged than the main highway itself. Thus, this option is disregarded in the analysis to follow, assuming that all vehicles will stay on the highway.

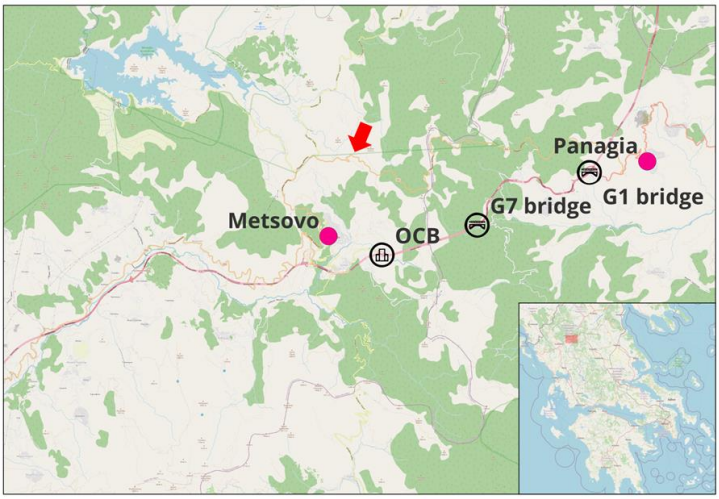

Figure 2. Metsovo-Panagia segment of the Egnatia highway in Greece showing the bridges of interest, the operator control building (OCB) and the alternative road (indicated by the red arrow).

Seismic hazard assessment

The seismic hazard is assessed for the Metsovo-Panagia segment via the OpenQuake platform (Pagani et al. 2014), by employing the area source model of the SHARE project (Giardini et al. 2013, Woessner et al. 2015) along with the ground motion equation of Boore and Atkinson (2008). Two Intensity Measures (IMs) are used in the analysis that are the peak ground acceleration, *PGA*, and the state-of-the-art average spectral acceleration, *AvgSa*, (Cordova et al. 2001, Vamvatsikos and Cornell 2005, Kazantzi and Vamvatsikos 2015):

$$AvgSa(T_{Ri}) = (\prod_{i=1}^{n} Sa(T_{Ri}))^{1/n} \quad (1)$$

It is the geometric mean of *n* spectral acceleration ordinates, *Sa*, at periods T_{Ri}. Each *Sa* ordinate is the geometric mean of the 5%-damped spectral acceleration from the two horizontal components of each ground motion. In our case, cotemporaneous damages and associated consequences need to be assessed for the entire highway, thus cotemporaneous values of the seismic hazard at all locations of interest should be determined. To achieve so, the seismic hazard is quantified in terms of event-based probabilistic seismic hazard analysis (event-based PSHA, Weatherill et al. 2015) that allows computing stochastic event sets (SES) of thousands of events that represent the seismicity of the region. In contrast to classical PSHA that provides an aggregated assessment of the seismic hazard, event-based analysis discretizes the hazard in events that allow determining spatially correlated IMs values at all locations of interest on an event basis. This enables assessing cotemporaneous damages for spatially distributed assets and makes event-based analysis the go-to option for seismic risk and resilience assessment especially in cases of interconnected systems, as is the highway network. An SES with an effective investigation period of 30,000 years is generated for the case at hand, whose ruptures are shown in Figure 3. For each rupture, the corresponding spatially correlated ground motion fields in terms of *PGA* and *AvgSa* are generated.

Seismic hazard disaggregation (Bazzurro and Cornell 1999, McGuire 2007) is also performed that allows identifying how different earthquake sources and magnitudes contribute to the seismic hazard. Disaggregation is performed in terms of *AvgSa* for three hazard levels, i.e., 20% probability of exceedance in 50years or 20%/50yrs, 10% probability of exceedance in 50 years or 10%/50yrs and 2% probability of exceedance in 50years or 2%/50yrs. The disaggregation analysis results for the 10%/50yrs hazard level are shown in Figure 4a, showing the contribution of different magnitude-distance-epsilon combinations to the seismic hazard, with epsilon being a measure of the deviation of the scenario value from the (logarithmic) mean of the ground motion prediction equation. The tallest bars indicate the magnitude/distance/epsilon combinations that contribute most to the seismic hazard. In this case, the seismic hazard tends to be controlled by nearby earthquakes, i.e., at distances lower than 15km. The mean disaggregation scenario is used as a basis for selecting three sets of 11 ground motion records, one per hazard level, that are compatible wit the site-specific hazard based on the Conditional Spectrum (Lin et al. 2013,

Kohrangi et al. 2017). The response spectra of the selected ground motion records as well as the conditional spectrum and with its 2.5, 50, and 97.5 percentiles are presented in Figure 4b.

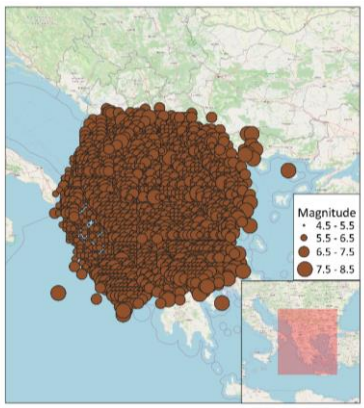

Figure 3. Stochastic event set for a duration of 30,000 years for the Metsovo-Panagia segment. Each circle represents a rupture, with its location indicating the epicenter and its diameter the moment magnitude.

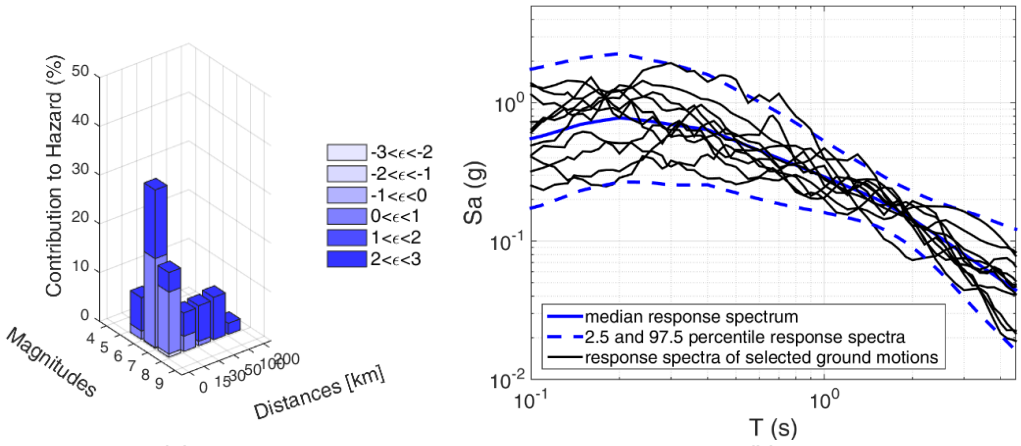

(a) (b)

Figure 4. (a) Disaggregation analysis results and (b) selected ground motion records for the 10%/50yrs hazard level.

Exposure model

Within the Metsovo-Panagia segment, the critical highway assets that are most vulnerable to the seismic hazard and are considered in the analysis are the G7 bridge, the G1 bridge, the Operator Control Building and the generic slopes around the highway.

G7 bridge

The G7 bridge consists of two structurally independent twin bridges, each of them carrying one traffic direction of two lanes, thus resulting in four lanes for both directions. The bridge was built in 2009 following the cantilever method of construction with in-situ concreting. Each of the bridges has three spans of 75+120+75m resulting in 270m total length. The longitudinal axis of the bridges is curved in both horizontal and vertical plane. The deck is a prestressed single-cell concrete box girder with its depth varying from 2.75m close to the abutments to 7.25m at the piers. The deck is monolithically connected to the two piers (M1 and M2) of 41.70m and 49.50 height, respectively. The cross section of both piers is hollow rectangular of in-situ cast concrete and is appropriately oriented so that deformation in the transverse bridge direction leads to bending around the cross-section strong-axis, while deformation in the longitudinal bridge direction leads to weak-axis bending. The piers are founded within the rock via concrete shafts of 10m diameter and 15m height. The deck is supported via two pot-bearings at each abutment that allow horizontal deck movements in both longitudinal and transverse bridge directions while a third bearing is added in the middle, having a transverse shear key to eventually restrict transverse bridge displacement until a controlled shear failure.

The critical components of the bridge that can sustain damage during earthquakes are the expansion joints, the bearings, the piers, the ballast wall and the deck ends. All these are carefully modelled within the three-dimensional model of the bridge developed by Vamvatsikos and Sigalas (2005) via the OpenSees software (Mazzoni et al. 2000), as shown in Figure 5. The model is subjected to multi-stripe analysis using the selected ground motion records and the response of all critical components is monitored during the analysis to allow assessing the damages and associated consequences to individual bridge components and then propagate them to asset-level performance.

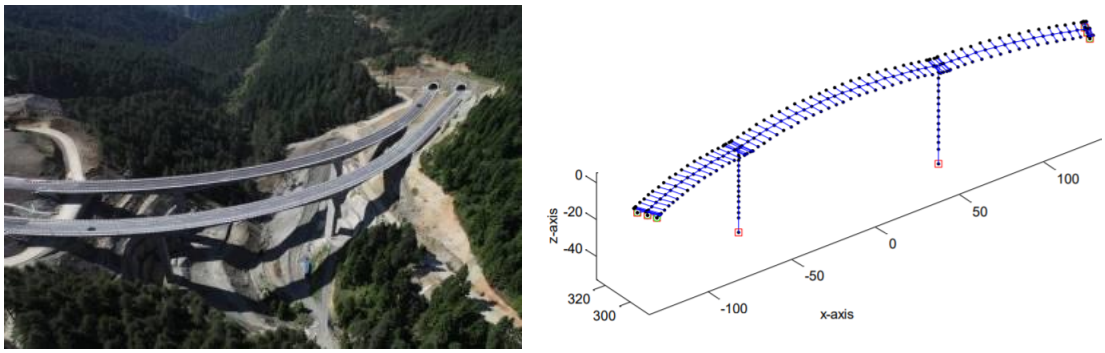

(a) (b)

Figure 5. (a) G7 bridge of Egnatia Odos and (b) three-dimensional model of the bridge (adopted from Giannelos and Vamvatsikos 2011).

G1 bridge

The G1 bridge consists of two structurally independent twin bridges, each carrying one traffic direction of two lanes, thus resulting in four lanes for both. The twin bridges were constructed in 2007; they have a total length of around 300m with spans of 37.5m (Figure 6a). The deck is a T-girder beam that is supported via elastometallic rubber bearings on the piers and the abutments. All piers are founded on deep foundations. These are mainly pile groups of 6-8 piles with 1.2m diameter, with the exception of three piles, one that lies within the area of a potential landslide and its two flanking ones; in this case, massive caissons are used. The potential landslide zone comprises an unstable relatively shallow soil layer, ranging from 8.5m to 10.5m depth, while the measured horizontal displacements indicate strain accumulation upon a thin zone of soil (slip plane). The critical components of the structure that can sustain seismic damage are the expansion joints, the piers, the bearings, and the foundation in the area of the landslide. They are modeled in detail by Mantakas et al. 2022 using the ABAQUS platform (Smith 2009) as shown in Figure 6b. The entire nonlinear model of soil, foundation, and bridge is subjected to MSA using the selected ground motion records. The response of all critical components is monitored in detail during the analysis and the results are used for assessing damages and associated consequences for all critical components as well as for the entire bridge-landslide system.

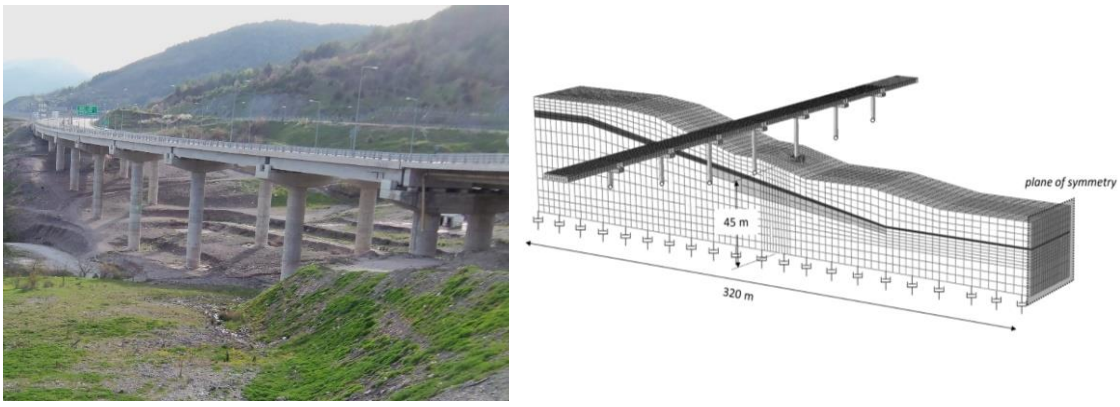

(a) (b)

Figure 6. (a) G1 bridge of Egnatia Odos and (b) finite element model of one of the twin bridges comprising the G1 bridge and of the active landslide (adopted from Mantakas et al. 2023).

Operator control building

The operation control building is located at Anilio and it is a 2-story reinforced concrete structure of 550m^2 covered area. It is vulnerable to the seismic hazard and potential damages after an event may have a disproportionate impact on the normal operation of the highway as it houses a Control Centre operating 24/7 with the following features:

- Monitors displaying real-time images from the different CCTV placed along the road corridor
- Telephone communication service 24/7
- Computer equipment including the data management tools

Figure 7. Operator control building.

Generic slopes around the highway

Within the Metsovo-Panagia segment many free slopes can be found. These can potentially be activated after an earthquake, resulting in soil falling on the highway thus disrupting its normal operation. For this reason, the regression model of Jibson (2007) is employed that relies on Newmark's method and allows assessing slope displacements for all events within the SES, based on the characteristics of each event.

Fragility and vulnerability assessment

Depending on the expected level of detail in the assessment, two approaches are followed for estimating the consequences per asset: (i) a component-based (FEMA P58-1 2012) and (ii) an asset-based treatment. The component-based approach allows differentiating the damages and consequences to individual asset components, while in the system-level treatment, system-level fragility curves are employed, such as the ones of HAZUS-MH (HAZUS 2012) that are combined with the cumulative consequences of the entire asset for the given damage state. The former enables a more detailed assessment than the latter. Influential assets, such as the G1 and G7 bridges receive a component-based treatment since any global rating of, e.g., "moderate damage" that might be triggered cannot be reliably traced back to individual bridge parts, which for the same level of damage might incur considerably different repair times and costs. On the contrary, the operator control building and the slopes receive a system-level treatment.

For the G1 and G7 bridges, the fragility and consequence functions are determined on a component-basis for all critical components based on expert opinion, while for the operator control building, generic fragility functions of HAZUS are adopted and are combined with expert-based consequences. For the slopes, fragility thresholds and consequence functions are determined based on expert opinion. For all assets/components, each damage state is associated to the expected losses, time to repair, number of lanes closed, and speed limit in the remaining open lanes. Going from the single asset to the entire system, repair actions are assumed to be performed in parallel for all assets; thus, system repair time is the maximum time needed for repairing all assets. Regarding speed, given the substantial length of tunnels comprising the Metsovo-Panagia segment, and the reluctance of highway operators to make lane adjustments within them, it is assumed that each lane has a constant speed limit across the entire segment that equals the minimum allowable speed limit imposed by the most critical damaged asset, as schematically shown in Figure 1b. Finally, the repair cost of the entire system is simply computed by aggregating the direct costs of all highway assets. Additional improvements could include post-event price-surge or volume discounts for large-level contracts vis-à-vis small-scale ones, but these are simple add-ons that are presently beyond the scope of the study.

The traffic delays associated to a potentially catastrophic event are assessed following a simplified approach as the limited length of the Metsovo-Panagia segment, low number of interchanges, and absence of alternative routes allow estimating traffic delays without employing more complex tools. Specifically, if the traffic demand is lower than the capacity, any potential reduction of the speed limit will cause delays associated with the reduced speed limit itself. Still, if the reduced capacity is close to the traffic demand, significant delays should be expected due to queueing, requiring additional time for each vehicle to traverse the highway. In this case, the delay per vehicle is determined by considering the time that a vehicle needs to traverse the highway while driving under the original speed versus the new time the vehicle needs, while additional delays due to queueing are approximated by employing the control delay of a vehicle approaching an unsignalized intersection per TRB (2000).

Example for a single scenario

The consequences and system recovery after a catastrophic event are determined for a seismic event that is randomly selected from the SES. Its magnitude is 6.3 and the location of its epicenter is shown in Figure 9a. The *PGA* and *AvgSa* ground motion fields are the ones shown in Figure 9b,c. The given event does not cause damages to the components of the G7 bridge (Figure 9a,b), while the slopes around the highway are not activated. Damages are expected to be observed at the expansion joints and the bearings at the abutments and the P1 pier of the G1 bridge (Figure 9c,d), plus the operator control building is slightly to moderately damaged (Figure 9e). Replacing/repairing the expansion joint requires closing one lane per direction and reducing the speed limit in the open one to 60km/h instead of its initial value of 80km/h, for approximately 35 days. When repair actions are finished, the speed limit is restored to its initial value and the normal operation of the highway is restored. The total cost needed for repairing all damages is estimated at 120,000€, allocated for repairing the expansion joint of the G1 bridge and the Operator Control Building. The response of the twin bridges comprising the G1 (termed G1Bridge_MP, G1Bridge_PM) and the G7 bridge (termed G7Bridge_MP, G7Bridge_PM) are assumed to be perfectly correlated, thus the travel restrictions (Figure 9f,g) are the same for both directions. Finally, the mean delay of a vehicle traversing the highway is expected to be 0.1h, assuming that demand is lower than the reduced capacity, which is the case for the highway currently. In cases when demand is higher than capacity, the expected traffic delays will be significantly higher.

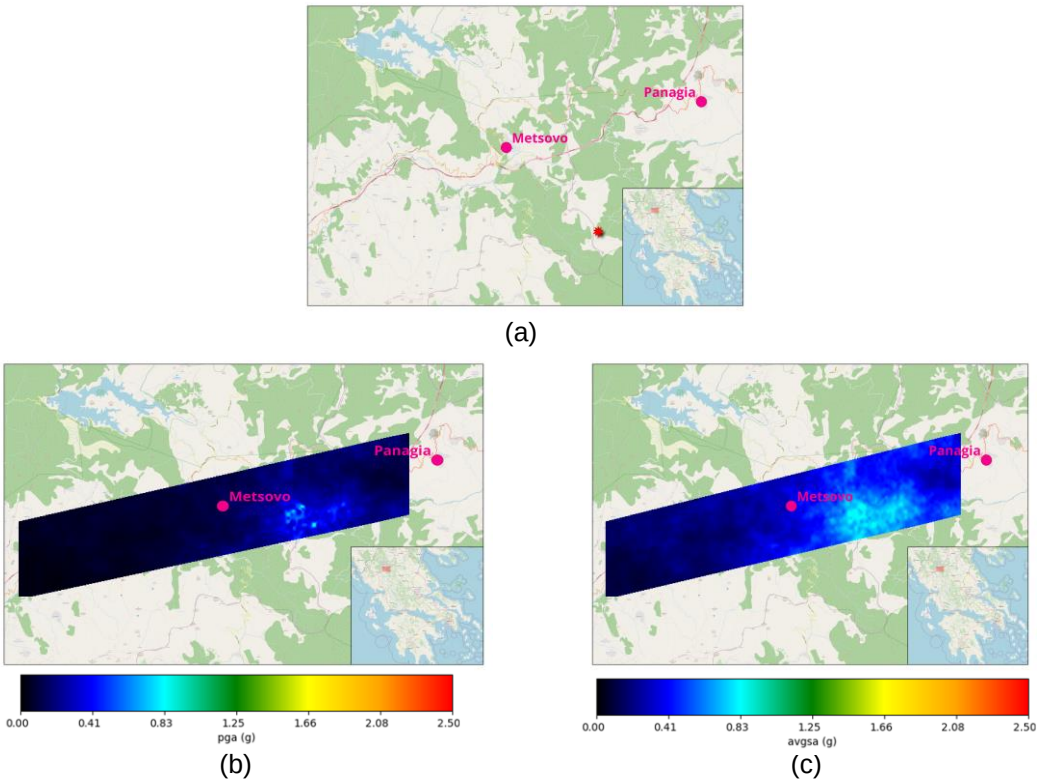

Figure 8. Ground motion fields for an earthquake of magnitude M6.3: (a) earthquake epicenter, (b) PGA ground motion field and (c) AvgSa ground motion field.

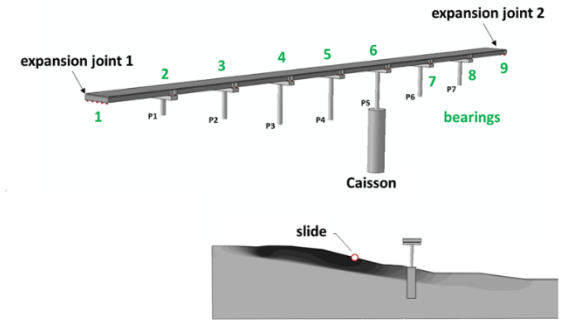

(a) components of the G1 bridge

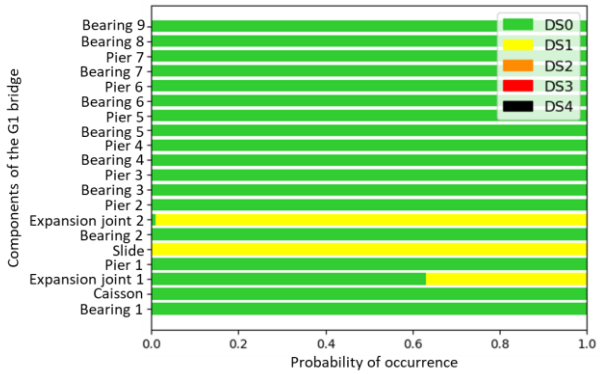

(b) damage state distribution for the components of the G1 bridge

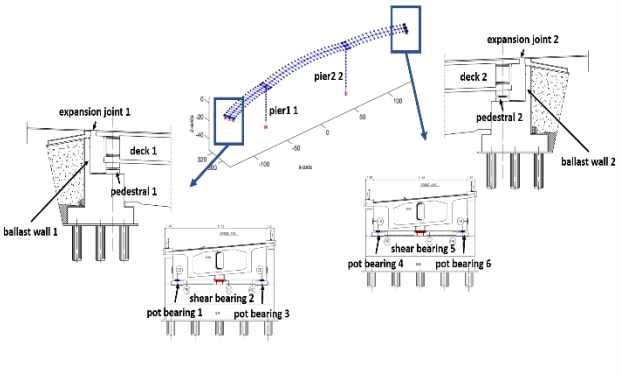

(c) components of the G7 bridge

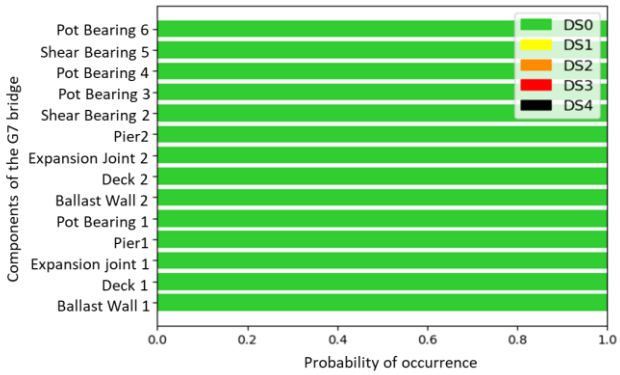

(d) damage state distribution for the components of the G7 bridge

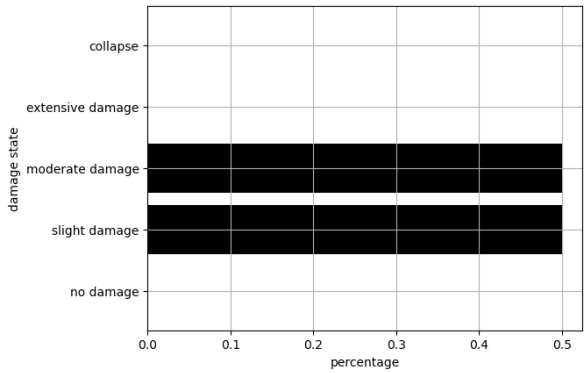

(e) damage state distribution for the operator control building

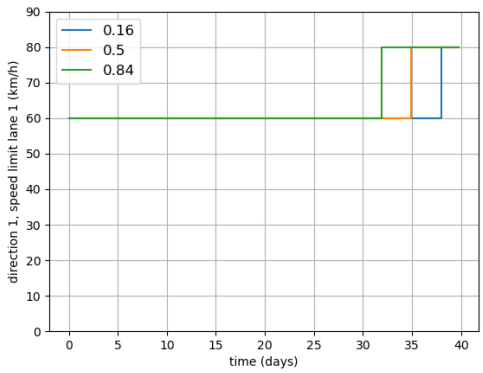

(f) recovery function of lane 1

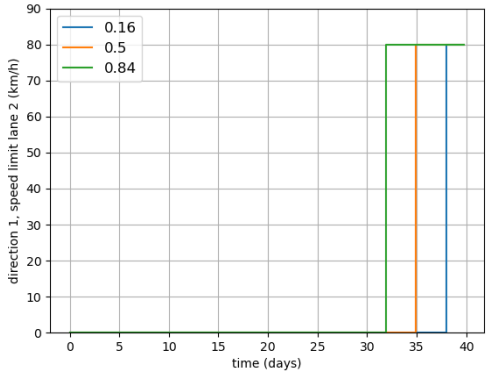

(g) recovery funtion of lane 2

Figure 9. Damages and associated consequences for the selected M6.3 seismic event.

Conclusions

Multiple levels of detail can be adopted when modeling the critical highway assets that need to be considered for assessing the risk and resilience of a highway, ranging from reduced-order models to highly detailed ones that can offer a comprehensive understanding of their response. Detailed models should be adopted for influential assets, while generic fragility and vulnerability functions can be used for less influential ones. Nowadays, the framework for assessing risk and resilience for the highway is quite straightforward, while the challenge is the definition of the limit states and the associated consequences on a component/asset basis. This requires the assistance of engineers specialized in the design and construction of similar structures as well as of road operators experienced in road maintenance, repair and rehabilitation actions. Once the damage states and consequences are defined, the consequences and resilience associated to any catastrophic event can be can be easily quantified.

Acknowledgments

This research has been financed by the European Commission through the Program "PLOTO – Deployment and assessment of predictive modelling, environmentally sustainable and emerging digital technologies and tools for improving the resilience of IWW against climate change and other extremes" with Grant Agreement number: 101069941 and the Hellenic Foundation for Research and Innovation (H.F.R.I.) under the “2nd Call for H.F.R.I. Research Projects to support Faculty Members & Researchers”, Project “TwinCity: Climate-Aware Risk and Resilience Assessment of Urban Areas under Multiple Environmental Stressors via MultiTiered Digital City Twinning” (Grant Agreement 2515).

References

Argyroudis SA, Mitoulis SA, Winter MG and Kaynia AM (2019), Fragility of transport assets exposed to multiple hazards: state-of-the-art review toward infrastructural resilience, *Reliability Engineering and System Safety*, 191, 106567.

Bazzurro P and Cornell CA (1999), Disaggregation of seismic hazard, *Bulletin of the Seismological Society of America*, 89(2), 501-520.

Boore DM and Atkinson GM (2008), Ground-motion prediction equations for the average horizontal component of PGA, PGV, and 5%-damped PSA at spectral periods between 0.01 s and 10.0 s, *Earthquake Spectra*, 24 (1), 99-138.

Chatzidaki A, Giannelos C, Gerontati A, Vamvatsikos D, Loli M and Tsatsis A (2022), Seismic risk and resilience assessment of the Metsovo-Panagia segment of the Egnatia Odos highway, *Proceedings of the 5th Panhellenic Conference on Earthquake Engineering and Engineering Seismology*, Athens, Greece COMPDYN2011.

Cimellaro GP, Reinhorn AM and Bruneau M (2006), Quantification of seismic resilience, Proceedings of the 8th US National conference on Earthquake Engineering.

Cimellaro GP, Reinhorn AM and Bruneau M (2010), Framework for analytical quantification of disaster resilience, *Engineering Structures*, 32, 3639-3649.

Cordova P, Deierlein G, Mehanny SF and Cornell CA (2001), Development of a two-parameter seismic intensity measure and probabilistic assessment procedure. *The Second U.S.-Japan Workshop on Performance-Based Earthquake Engineering Methodology for Reinforced Concrete Building Structures*, Sapporo, Hokkaido, Japan.

Cornell CA and Krawinkler H (2000), Progress and challenges in seismic performance assessment, *PEER Center News*, 3, 1-4.

Costa CQ (2018), Impact of earthquakes due to disruption in transportation networks using open tools and datasets, *PhD thesis*, University of Pavia, Italy.

FEMA P58-1 (2012), Seismic performance assessment of buildings: 1–Methodology, Prepared by the Applied Technology Council for the Federal Emergency Management Agency.

Giannelos C and Vamvatsikos D (2011), Simplified seismic performance assessment over the lifetime of a highway bridge subject to pier reinforcement corrosion. *Proceedings of the COMPDYN2011 Conference on Computational Methods in Structural Dynamics and Earthquake Engineering*, Corfu, Greece.

Giardini D, Woessner J, Danciu L, Crowley H, Cotton F, Grünthal G, et al. (2013), Seismic Hazard Harmonization in Europe (SHARE): Online Data Resource, http://www.share-eu.org/node/61.html.

Hazus (2012), *Hazus–MH 2.1: Technical manual*. Washington, DC, USA

Jalayer F and Cornell CA (2009), Alternative non-linear demand estimation methods for probability-based seismic assessments, *Earthquake Engineering and Structural Dynamics*, 38(8), 776 951–972.

Jibson RW (2007), Regression models for estimating coseismic landslide displacement, *Engineering Geology*, 91(2-4), 209-218

Kappos A, Sextos A, Stefanidou S, Mylonakis G, Pitsiava M and Sergiadis G (2014), Seismic risk of inter-urban transportation networks, *Procedia Economics and Finance*, 18, 263-270

Kazantzi AK and Vamvatsikos D (2015), Intensity measure selection for vulnerability studies of building classes, E*arthquake Engineering and Structural Dynamics*, 44(15), 2677-2694.

Kilanitis I and Sextos A (2019), Integrated seismic risk and resilience assessment of roadway networks in earthquake prone areas, *Bulletin of Earthquake Engineering*, 17, 181-210.

Kohrangi M, Bazzurro P, Vamvatsikos D and Spillatura A (2017), Conditional spectrum-based ground motion record selection using average spectral acceleration, *Earthquake Engineering and Structural Dynamics*, 46(10), 1667-1685.

Lin T, Haselton CB and Baker JW (2013), Conditional spectrum-based ground motion selection. Part I: Hazard consistency for risk-based assessments, *Earthquake Engineering and Structural Dynamics*, 42(12), 1847-1865.

Mantakas A, Tsatsis A, Loli M, Kourkoulis R and Gazetas G (2022), Seismic response of a motorway bridge founded in an active landslide: a case study, *Bulletin of Earthquake Engineering*, 21(1), 605-632. DOI: 10.1007/s10518-022-01544-3

Mazzoni S, McKenna F, Scott M and Fenves G (2000), Open system for earthquake engineering simulation: OpenSees command language manual, University of California, Berkeley, CA, 2000.

McGuire RK (2007), Probabilistic seismic hazard analysis: Early history. *Earthquake Engineering and Structural Dynamics*, 37(3), 329-338.

Miles SB and Chang SE (2006), Modeling community recovery from earthquakes, *Earthquake Spectra* 22(2), 439-458.

Ouyang M, Dueñas-Osorio L and Min X (2012), A three-stage resilience analysis framework for urban infrastructure systems, *Structural Safety*, 36-37, 23-31.

Pagani M, Monelli D, Weatherill GA and Garcia J (2014), *The OpenQuake-engine Book: Hazard*. Global earthquake model (GEM) technical report 2014-08.

Smith M (2009), *ABAQUS/Standard User's Manual*, Version 6.9. Providence, RI: Dassault Systèmes Simulia Corp.

TRB (2000), *Highway Capacity Manual 2000* (HCM 2000), National Research Council, Transportation Research Board.

Vamvatsikos D and Cornell CA (2005), Developing efficient scalar and vector intensity measures for IDA capacity estimation by incorporating elastic spectral shape information, *Earthquake Engineering and Structural Dynamics*, 34(13), 1573-1600.

Vamvatsikos D and Sigalas I (2005), Seismic performance evaluation of a horizontally curved highway bridge using incremental dynamic analysis in 3D, *Proceedings of the 4th European Workshop on the seismic behaviour of irregular and complex structures*, Thessaloniki, Greece.

Weatherill G, Silva V, Crowley H and Bazzurro P (2015), Exploring the impact of spatial correlations and uncertainties for portfolio analysis in probabilistic seismic loss estimation. *Bulletin of Earthquake Engineering*, 13, 957-981.

Woessner J, Danciu L, Giardini D, Crowley H, Cotton F, Grünthal G et al. (2015), The 2013 European seismic hazard model: key components and results, *Bulletin of Earthquake Engineering*, 13(12), 3553–3596.

Zhang W, Wang N and Nicholson C (2017), Resilience-based post-disaster recovery strategies for road-bridge networks, *Structure and Infrastructure Engineering*, 13(11), 1404-1413.